

Helical Chirality Induction by Point Chirality at Helix Terminal

Tadashi Mizutani,* Shigeyuki Yagi,† Tomoko Morinaga,† Tetsutaro Nomura,† Toru Takagishi,† Susumu Kitagawa, and Hisanobu Ogoshi‡

Contribution from the Department of Synthetic Chemistry and Biological Chemistry, Graduate School of Engineering, Kyoto University, Yoshida, Sakyo-ku, Kyoto 606-8501 Japan, Department of Applied Materials Science, Osaka Prefecture University, Gakuen-cho, Sakai, Osaka 599-8531 Japan, and Fukui National College of Technology, Geshi, Sabae, Fukui 916-0064 Japan

Received August 27, 1998

Abstract: A series of zinc bilinone derivatives bearing a chiral auxiliary at the helix terminal were prepared to investigate the helical chirality induction in the bilinone framework by the point chirality of the chiral auxiliary. Chiral induction was sensitive to the distance to the asymmetric carbon as well as to substituents on the asymmetric carbon. When the chiral carbon was directly attached to the bilinone 19-oxygen and carried an aromatic group, relatively high helical chirality induction was observed in [19-alkoxy-2,7,13,18-tetramethyl-3,8,12,17-tetraethyl-1-bilinonato]zinc(II) as demonstrated by variable-temperature ^1H NMR and CD studies. The (*R*)-2-methyl-1-phenylpropanoxy group induced *P*-helicity in >95% enantiomeric excess at 223 K in CD_2Cl_2 ($\Delta\Delta G^\circ \geq 6.8$ kJ/mol).

Introduction

Point chirality of an organic molecule emerges if four different substituents are attached to a single carbon. The point chirality is fundamental and seen even in simple small molecules. If it is integrated into helical chirality, several interesting functions will arise such as unidirectional motion of a molecule.¹ In this context, point chirality–helical chirality interconversion is of great importance and interest to understand structural features of chiral functional molecules including biomolecules² as well as to design a wide range of stereoselective processes such as asymmetric synthesis³ and enantiomer separation.⁴ Topologically, there are two geometrically different orientations of point chirality relative to helical chirality: one is to place point chirality on the helix axis (Figure 1a), and the other is to place point chirality on the side of helix (Figure 1b).⁵

Metal complexes of bilinones are a unique class of compounds having helical chirality in themselves. Functional groups can be introduced both at the metal center as a ligand and at peripheral positions as substituents. Therefore, there is a

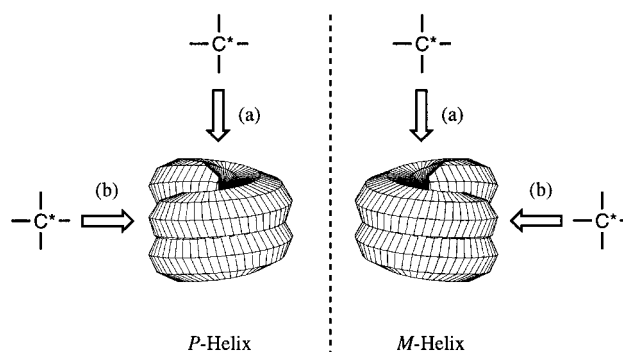


Figure 1. Two geometries of point chirality relative to helical chirality. (a) Point chirality on the helix axis and (b) on the side of helix.

possibility of controlling the chirality of the helix of bilinone by designing the structures of ligand and substituent. We previously reported that point chirality of amino acid esters placed on the helix axis (Figure 1a) as a ligand induced helical chirality in zinc bilinone through a combination of noncovalent interactions.⁶ As another approach, introduction of chiral groups at the pyrrole β -position was reported,⁷ giving rise to only small helical chirality induction. One remarkable feature of bilinone chemistry is the reversible equilibrium between oxoniaporphyrin and bilinone as typically shown for the zinc complexes in Scheme 1.^{8,9} This reaction also provides a facile synthetic route to bilinone derivatives with various alkoxy groups at the D-ring.

(6) (a) Mizutani, T.; Yagi, S.; Honmaru, A.; Ogoshi, H. *J. Am. Chem. Soc.* **1996**, *118*, 5318–5319. (b) Mizutani, T.; Yagi, S.; Honmaru, A.; Murakami, S.; Furusyo, M.; Takagishi, T.; Ogoshi, H. *J. Org. Chem.* **1998**, *63*, 8769–8784.

(7) (a) Lehner, H.; Riemer, W.; Schaffner, K. *Liebigs Ann. Chem.* **1979**, 1798–1801. (b) Boiadjev, S. E.; Anstine, D. T.; Lightner, D. A. *Tetrahedron: Asymmetry* **1995**, *6*, 901–912.

(8) (a) Fuhrhop, J.-H.; Salek, A.; Subramanian, J.; Mengersen, C.; Besecke, S. *Liebigs Ann. Chem.* **1975**, 1131–1147. (b) Fuhrhop, J. H.; Krueger, P. *Justus Liebigs Ann. Chem.* **1977**, 360–70. (c) Falk, H.; Grubmayr, K.; Thirring, K. *Z. Naturforsch.* **1978**, *33b*, 924–931.

(9) Latos-Grazynski, L.; Johnson, J.; Attar, S.; Olmstead, M. M.; Balch, A. L. *Inorg. Chem.* **1998**, *37*, 4493–4499.

* Corresponding Author. Kyoto University. Telephone number: 81-75-753-5662. Fax number: 81-75-753-4979. E-mail: mizutani@sbchem.kyoto-u.ac.jp.

† Osaka Prefecture University.

‡ Fukui National College of Technology.

(1) Gilat, G. *J. Phys. A: Math. Gen.* **1989**, *22*, L545–L550.

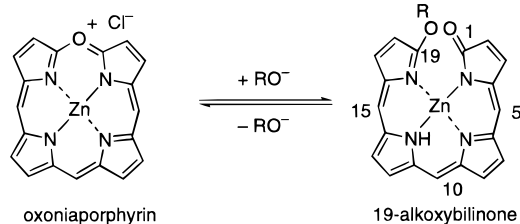
(2) For examples of interactions between different kinds of chirality, see: Lightner, D. A.; Gawronski, J. K.; Gawronska, K. *J. Am. Chem. Soc.* **1985**, *107*, 2456–2461; Yashima, E.; Matsushima, T.; Okamoto, Y. *J. Am. Chem. Soc.* **1997**, *119*, 6345–6359; Obata, K.; Kabuto, C.; Kira, M. *J. Am. Chem. Soc.* **1997**, *119*, 11345–11346; Kano, K.; Negi, S.; Kamo, H.; Kitae, T.; Yamaguchi, M.; Okubo, H.; Hirama, M. *Chem. Lett.* **1998**, 151–152.

(3) Reetz, M. T.; Beuttenmüller, E. W.; Goddard, R. *Tetrahedron Lett.* **1997**, *38*, 3211–3214.

(4) Pirkle, W. H.; Pochapsky, T. C. *J. Am. Chem. Soc.* **1987**, *109*, 5975–5982; Okamoto, Y.; Kawashima, M.; Harada, K. *J. Am. Chem. Soc.* **1984**, *106*, 5357–5359.

(5) For examples of noncovalent interactions with helical chirality, see: (a) Green, M. M.; Peterson, N. C.; Sato, T.; Teramoto, A.; Cook, R.; Lifson, S. *Science* **1995**, *268*, 1860–1866. (b) Konishi, K.; Kimata, S.-i.; Yoshida, K.; Tanaka, M.; Aida, T. *Angew. Chem., Int. Ed. Engl.* **1996**, *35*, 2823–2825.

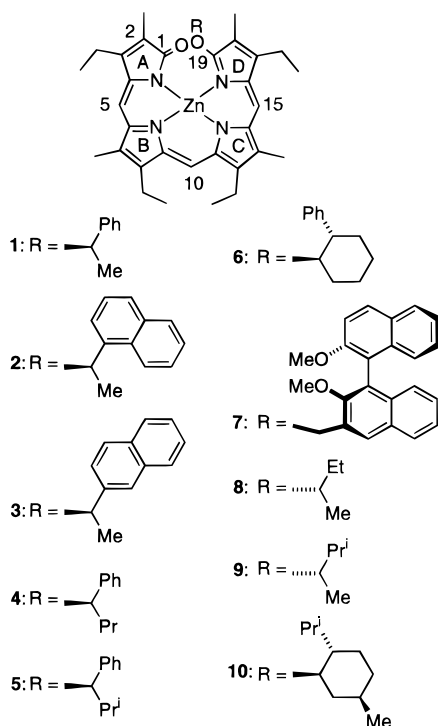
Scheme 1



We describe here the synthesis of novel chiral zinc bilinones bearing point chirality at the D-ring, focusing on the efficiency of helical chirality induction in the bilinone framework by the point chirality attached to its helix terminal.^{10,11}

Results and Discussion

Preparation of Zinc Bilinones Bearing Point Chirality at Helix Terminal. Chiral zinc bilinones **1–10** were prepared by



a ring-cleavage reaction of [5-oxoniaporphyrinato]zinc(II) chloride (**11**) with chiral alkoxides in THF to give free bases of **1–10**.⁸ Zinc(II) was inserted to afford **1–10** in 27–41% yields from **11** after purification by gel permeation chromatography. The structures were identified by the ¹H NMR spectra and high-resolution FAB mass spectra. The ¹H–¹H NOESY spectra showed correlation peaks between 5-, 10-, 15-protons and their neighboring methyl and/or methylene protons, indicating that the molecules adopt a (*Z,Z,Z*) helical conformation.

Helical Chirality Induction in Bilinone Framework. Circular dichroism spectra of **1–6** and **9–10** in CH₂Cl₂ showed characteristic patterns of a chiral helical framework of bilinone.

(10) Helical chirality induction in bilindione by proteins, see: Huber, R.; Schneider, M.; Mayr, I.; Muller, R.; Deutzmann, R.; Suter, F.; Zuber, H.; Falk, H.; Kayser, H. *J. Mol. Biol.* **1987**, *198*, 499–513; Wagner, U. G.; Muller, N.; Schmitzberger, W.; Falk, H.; Kratky, C. *J. Mol. Biol.* **1995**, *247*, 326–337.

(11) Helical chirality induction in bilindione by covalently attached peptide, see: Krois, D.; Lehner, H. *J. Chem. Soc., Perkin Trans. 2* **1987**, 1523–1526; Micura, R.; Grubmayr, K. *Angew. Chem., Int. Ed. Engl.* **1995**, *34*, 1733–1735.

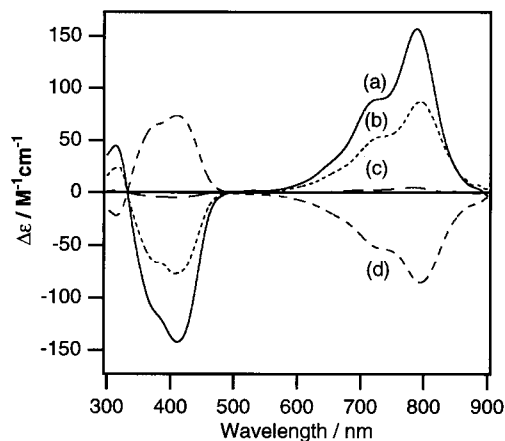


Figure 2. Circular dichroism spectra of (a) (*R*)-**5**, (b) (*R*)-**1**, (c) (*S*)-**8**, and (d) (*S*)-**1** in CH₂Cl₂ at 288 K.

As shown in Figure 2, (*R*)-**1** and (*R*)-**5** exhibited a negative Cotton effect at 400 nm and a positive one at 700–800 nm, revealing that *P*-helicity is dominant in the bilinone framework.¹² The values of $\Delta\epsilon$ and the induced helical chirality at 288 and at 223 K are listed in Table 1. Scheme 2 shows the equilibrium between the two diastereomers, *P*-form and *M*-form, which is responsible for the observed Cotton effects.

The ¹H NMR spectra of **1–10** in CD₂Cl₂ at 288 K exhibited two sets of signals either with unequal intensities (**1–6** and **10**) or with almost equal intensities (**7–9**). Similar spectral patterns were observed at 223 K, although the ratios of the major signals to the minor ones were larger at 223 K. These signals were ascribed to the two diastereomers, one with *P*-bilinone and the other with *M*-bilinone (see Scheme 2), with the major signals of **1–6** and **10** assigned to the former diastereomer based on the sign of the Cotton effects. Therefore the helix inversion between *P*- and *M*-helix was slow on the ¹H NMR time scale at 288 K for **1–10**. The efficiency of helical chirality induction can be directly determined by integration of signals of the major diastereomers and the minor ones. Diastereomeric excesses of **1–10** at 288 and 223 K determined from the signal integration are listed in Table 1. By attaching a simple chiral group such as the (*R*)-1-phenylethoxy group (**1**) or the (1*R*,2*S*)-2-phenylcyclohexanooxy group (**6**), a relatively high diastereomeric excess was obtained. The zinc bilinone bearing the (*R*)-2-methyl-1-phenylpropoxy group (**5**) showed almost exclusive formation of *P*-helix at 223 K. On the other hand, helical chirality was not induced by a binaphthyl moiety attached through a methylene linkage as seen in 0% de of **7**. The diastereomeric excesses of **8** and **9** were also small, showing that a simple aliphatic chiral auxiliary was inefficient in helical chirality induction. Efficiency of helical chirality induction was thus sensitive to the distance to the asymmetric carbon as well as the substituents on the asymmetric carbon.

Molecular Modeling Study. It is noteworthy that, for aromatic auxiliaries, bulkiness of the aromatic group does not affect the chiral induction much (similar diastereomeric excesses for both phenyl and naphthyl auxiliaries, **1** vs **2** and **3**), while the bulkiness of the aliphatic group significantly affects the chiral

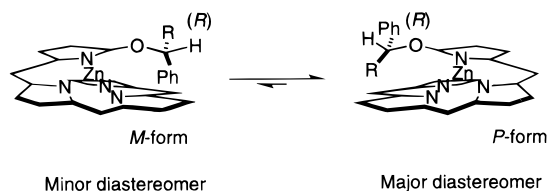
(12) (a) Bulke, M. J.; Pratt, D. C.; Moscovitz, A. *Biochemistry* **1972**, *11*, 4025–4031. (b) Chae, Q.; Song, P. S. *J. Am. Chem. Soc.* **1975**, *97*, 4176–4179. (c) Blauer, G.; Wagniere, G. *J. Am. Chem. Soc.* **1975**, *97*, 1949–1954. (d) Wagniere, G.; Blauer, G. *J. Am. Chem. Soc.* **1976**, *98*, 7806–7810. (e) Sugimoto, T.; Ishikawa, K.; Suzuki, H. *J. Phys. Soc. Jpn.* **1976**, *40*, 258. (f) Falk, H.; Hollbacher, G. *Monatsh. Chem.* **1978**, *109*, 1429. (g) Scheer, H.; Formanek, H.; Schneider, S. *Photochem. Photobiol.* **1982**, *36*, 259–272. (h) Krois, D.; Lehner, H. *J. Chem. Soc., Perkin Trans. 2* **1993**, 1837–1840.

Table 1. Differential Dichroic Absorptions ($\Delta\epsilon$) in the CD Spectra and Diastereomeric Excesses for **1–10** in Dichloromethane at 288 K and 223 K

	$\Delta\epsilon/M^{-1} \text{ cm}^{-1} (\lambda/\text{nm}, \text{helicity})$		de (%) ^a	
	288 K	223 K	288 K	223 K
(<i>R</i>)- 1	−76.7 (410, <i>P</i>), 87.4 (794)	−106.0 (403, <i>P</i>), 120.9 (783)	60	81
(<i>R</i>)- 2	−97.3 (412, <i>P</i>), 96.9 (805)	−126.8 (406, <i>P</i>), 127.8 (792)	69	84
(<i>R</i>)- 3	−89.8 (409, <i>P</i>), 107.2 (796)	−124.2 (403, <i>P</i>), 152.4 (780)	69	85
(<i>R</i>)- 4	−96.7 (411, <i>P</i>), 103.7 (791)	−114.5 (403, <i>P</i>), 123.7 (777)	74	86
(<i>R</i>)- 5	−142.1 (412, <i>P</i>), 156.9 (788)	−152.6 (402, <i>P</i>), 170.3 (770)	95	>95
(1 <i>R</i> ,2 <i>S</i>)- 6	−65.2 (405, <i>P</i>), 94.6 (800)	−88.2 (402, <i>P</i>), 137.8 (787)	51	72
7		6.3 (413, <i>M</i>), −5.0 (763)	ca. 0	ca. 0
(<i>S</i>)- 8	−13.2 (410, <i>P</i>), 14.2 (774)	−7.2 (414, <i>P</i>), 9.4 (750)	1	3
(<i>S</i>)- 9	−21.6 (406, <i>P</i>), 23.7 (774)	−4.0 (424), 4.3 (680), 13.7 (750), −17.5 (788)	7	7
10	85.0 (411, <i>M</i>), −104.5 (777)	99.0 (402, <i>M</i>), −130.2 (758)	46	48

^a Determined by ¹H NMR integration of each signal of the diastereomers.

Scheme 2



induction as seen from the comparison of diastereomeric excess of **1** and of **5**. These observations indicated that the bulk of the aromatic group does not have particular effects on helical chirality induction and that the bulk of the aliphatic group does affect it. Molecular modeling studies using conformational search and ab initio molecular orbital calculations supported these observations. A grid search for stable conformers of a model compound of **5** was performed¹³ by varying the two dihedral angles, N–C(19)–O(19)–C(chiral) and C(19)–O(19)–C(chiral)–C(phenyl), based on the force field calculations. The geometry of the stable conformers was further optimized at the HF/3-21G* level.¹⁴ Figure 3 shows four selected conformers, a and b, *R–P* major diastereomers, and c and d, *R–M* minor diastereomers. In the most stable conformer a, the phenyl group points away from the bilinone framework, and the methyl group of the isopropyl group and the A-ring are in van der Waals contact (the methyl proton–C(3) distance was 2.95 Å). In the *R–M* isomer with an unfavorable combination of chirality, the most stable one was conformer c, in which the phenyl group is closer to the A-ring. These molecular modeling studies showed that the van der Waals interaction between the isopropyl group and the A-ring stabilized the major diastereomer complex, consistent with the experimental observation that changes in the size of the alkyl group significantly affected the efficiency of helical chirality induction.

Correlation between Cotton Effects and Diastereomeric Excesses. Except for **8**, **9**, and **10**, a linear correlation was found between the values of $|\Delta\epsilon|_{\text{max}}$ of the higher-energy band of the CD spectra and diastereomeric excesses determined by ¹H NMR studies (Figure 4). The slope of the line, α , for the chiral bilinones **1–7** is 1.38, quite similar in magnitude to that obtained

(13) A model compound, in which 3,7,8,12,13,16-alkyl groups of **5** are replaced by hydrogens, was used. Grid search was performed by use of Sybyl 6.1, Tripos Inc.

(14) Frisch, M. J.; Trucks, G. W.; Schlegel, H. B.; Gill, P. M. W.; Johnson, B. G.; Robb, M. A.; Cheeseman, J. R.; Keith, T.; Petersson, G. A.; Montgomery, J. A.; Raghavachari, K.; Al-Laham, M. A.; Zakrzewski, V. G.; Ortiz, J. V.; Foresman, J. B.; Cioslowski, J.; Stefanov, B. B.; Nanayakkara, A.; Challacombe, M.; Peng, C. Y.; Ayala, P. Y.; Chen, W.; Wong, M. W.; Andres, J. L.; Replogle, E. S.; Gomperts, R.; Martin, R. L.; D. J. Fox; Binkley, J. S.; Defrees, D. J.; Baker, J.; Stewart, J. P.; Head-Gordon, M.; Gonzalez, C.; Pople, J. A. *Gaussian 94, Revision E.2* Pittsburgh, PA, 1995.

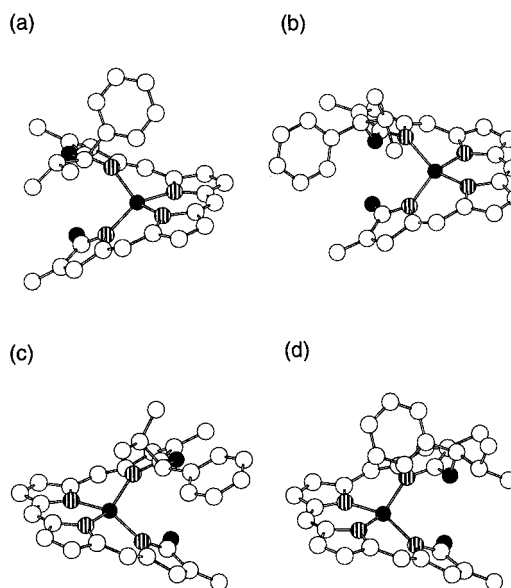


Figure 3. Possible conformers of a model compound for **5**. All of the peripheral alkyl groups at the β -position of pyrroles were replaced with hydrogens except for the 2-methyl and 18-methyl groups. The geometry was optimized at the HF/3-21G* level. Hydrogen atoms are omitted for clarity. (a) *R*-**5**-*P*-helix with the phenyl group pointed upward, $E = -3318.3694$ au, (b) *R*-**5**-*P*-helix with the phenyl group positioned on the outside of the helix, $E = -3318.3585$ au, (c) *S*-**5**-*P*-helix with the phenyl group tilted toward the A-ring of bilinone, $E = -3318.3656$ au, and (d) *S*-**5**-*P*-helix with the phenyl group directed upward, $E = -3318.3618$ au. Relative energy increases in the order (a) $0 < (c)$ $2.4 < (d)$ $4.8 < (b)$ 6.8 kcal/mol.

for the amino ester-zinc 19*O*-methylbilinone ($\alpha = 1.22$),⁶ although the zinc of the former complex is four-coordinated and that of the latter is five-coordinated. These results indicate that the conformation of bilinone framework is similar between the two systems, and the magnitude of the Cotton effects for both systems is dominated by the relative ratio of *P*- and *M*-enantiomers of bilinones. Deviation of compounds **8–10** from the linear correlation indicates that these molecules may adopt a somewhat different conformation.

Conclusion

We have shown that helical chirality of zinc bilinones can be controlled by attaching a simple chiral group at the helix terminal. Direct connection of the asymmetric carbon to the oxygen of bilinone as well as substitution of the aromatic group and the aliphatic moiety of suitable size on the asymmetric carbon greatly assisted the helical chirality induction, leading to diastereomeric excess higher than 95%.

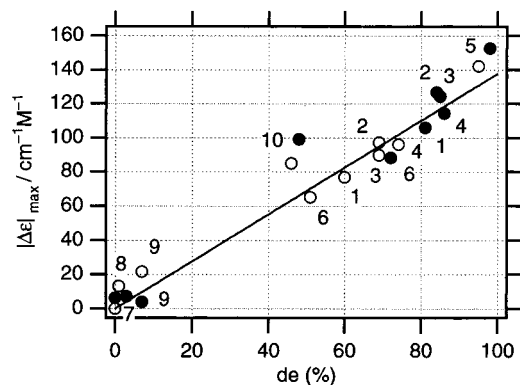


Figure 4. Plot of $|\Delta\epsilon|_{\max}$ in the higher-energy band against diastereomeric excesses for **1–10** at 288 K (○) and at 223 K (●). A line was drawn by least-squares line fitting to data except **8, 9**, and **10**: $|\Delta\epsilon|_{\max} = 1.38 \times de$.

Experimental Section

General Methods. ^1H NMR spectra (500 MHz) were recorded in CDCl_3 and CD_2Cl_2 , using TMS (0 ppm) and CH_2Cl_2 (5.32 ppm) as internal standards, respectively. ^{13}C NMR spectra (125.7 MHz) were recorded in CDCl_3 , using TMS (0 ppm) as an internal standard. UV-vis absorption and circular dichroism spectra were recorded on the spectrometers equipped with a thermostated cell compartment. Low-temperature circular dichroism spectra were recorded on the spectrometer equipped with an Oxford DN1704 cryostat. For the preparation of sample solutions for spectroscopic measurements, dichloromethane solutions of zinc bilinones or guests were prepared in a volumetric flask at 15 °C, and the concentrations at low temperatures were corrected on the basis of the thermal expansion coefficient of dichloromethane (0.001391 K^{-1}).¹⁵ FAB mass spectra were obtained using 3-nitrobenzyl alcohol as a matrix. The optical rotation of (*R*)-2,2'-dimethoxy-1,1'-binaphthalen-3-ylmethanol was recorded using a polarimeter with a sodium lamp (D-line, 589 nm) as a light source. Gel permeation chromatography was performed on an HPLC by connecting SHODEX GPC K-2001 and 2002 poly(styrene) gel column packages successively, where CHCl_3 was used as eluent.

Materials and Solvents. (2,8,13,17-Tetraethyl-3,7,12,18-tetramethyl-5-oxoniaporphyrinato)zinc(II) chloride (**11**) was prepared by the procedure reported previously.^{6b} All chiral alcohols except (*R*)-2,2'-dimethoxy-1,1'-binaphthalen-3-ylmethanol were purchased and used without further purification. (*R*)- and (*S*)-1-Phenylethanol, and (1*R*,2*S*,5*R*)-5-methyl-2-isopropyl-1-cyclohexanol (L-(−)-menthol) were purchased from Wako Pure Chemicals Industries. (*R*)-1-(1-Naphthyl)ethanol, (*R*)-1-(2-naphthyl)ethanol, (*R*)-1-phenyl-1-butanol, (*R*)-2-methyl-1-phenyl-1-propanol, (*S*)-3-methyl-2-butanol, and (*S*)-3-methyl-2-butanol were purchased from Aldrich. (1*R*,2*S*)-2-Phenyl-1-cyclohexanol was purchased from AZmax Co. Ltd. THF and diethyl ether used for syntheses were dried over LiAlH_4 at reflux and distilled under Ar prior to use. Dichloromethane of spectroscopic grade was purchased from Nacalai Tesque, Inc. for UV-vis and CD studies.

(*R*)-2,2'-Dimethoxy-1,1'-binaphthalen-3-ylmethanol. To a solution of (*R*)-2,2'-dimethoxy-1,1'-binaphthalene (0.629 g, 2.00 mmol)¹⁶ in dry ether (25 mL) was added under Ar *n*-BuLi (1.57 M in hexane, 5.10 mL, 8.01 mmol), and the mixture was refluxed for 18 h. To the mixture was added in one portion paraformaldehyde (0.601 g, 20.0 mmol), and the solution was refluxed for 3 h. After the mixture was cooled, the solvent was removed by evaporation, and to the residue was added 1 M HCl (50 mL). The product was taken up in CH_2Cl_2 (50 mL), and the organic layer was washed with water (50×2 mL) and saturated brine (50 mL), dried over anhydrous MgSO_4 , and evaporated in vacuo. The residue was purified by silica gel column chromatography (hexane/ $\text{CH}_2\text{Cl}_2 = 1/1$ (v/v) as eluent) to afford a white solid of the desired

product (77.0 mg, 0.224 mmol, 11%): mp 78–82 °C; ^1H NMR (500 MHz, CDCl_3) δ 1.93 (br s, 1H), 3.39 (s, 3H), 3.80 (s, 3H), 4.91 (d, $J = 13.1$ Hz, 1H), 4.99 (d, $J = 13.1$ Hz, 1H), 7.11–7.13 (m, 2H), 7.20–7.26 (m, 2H), 7.31–7.40 (m, 2H), 7.47 (d, $J = 9.2$, 1H), 7.87–7.88 (m, 2H), 7.94 (s, 1H), 8.02 (d, $J = 9.2$, 1H); ^{13}C NMR (125.7 MHz, CDCl_3) δ 56.54, 60.66, 62.66, 113.48, 118.88, 123.71, 124.48, 124.89, 125.16, 125.32, 126.12, 126.77, 127.85, 127.93, 127.95, 129.04, 129.97, 130.62, 133.64, 133.77, 133.94, 154.66, 154.91; IR (KBr) 3392, 1593, 1506, 1400, 1356, 1265, 1244, 1103, 1080, 1018, 810, 752 cm^{-1} ; EI MS m/z 344 ($[\text{M}]^+$); HR EI MS calcd for $[\text{C}_{23}\text{H}_{20}\text{O}_3]^+$ 344.1412, found 344.1418. Anal. Calcd for $\text{C}_{23}\text{H}_{20}\text{O}_3$: C, 80.21; H, 5.85. Found: C, 80.19; H, 5.77; $[\alpha]_D^{25} +121.7^\circ$ (c 0.136, CH_2Cl_2).

[3,8,12,17-Tetraethyl-1,21-dihydro-2,7,13,18-tetramethyl-19-((*R*)-1-phenylethoxy)-(21*H*,24*H*)-1-bilinonato(2-)- $N^{21},N^{22},N^{23},N^{24}$]zinc(II) ((*R*)-1**).** A mixture of NaH (60% oil dispersion, 22.5 mg, 0.563 mmol) and (*R*)-1-phenylethanol (53.4 mg, 0.437 mmol) in dry THF (10 mL) was stirred at room temperature for 30 min. To the reaction mixture was added (5-oxoniaporphyrinato)zinc(II) chloride **11** (120 mg, 0.207 mmol), and the resultant solution was stirred for 12 h. The solvent was removed by evaporation, and CH_2Cl_2 (50 mL) was added to the residue, followed by washing with 10% NH_4Cl (50 mL). The organic layer was vigorously shaken with a phthalate buffer solution (pH = 4.0, 50 mL \times 3), where the dark-green solution turned blue. The organic layer was washed with water (50 mL) and saturated brine (50 mL). After the mixture was dried over anhydrous Na_2SO_4 , the solvent was removed by evaporation. Purification of the residue by silica gel column chromatography ($\text{CH}_2\text{Cl}_2/\text{MeOH} = 100/1$ (v/v) as eluent) afforded a dark-blue solid, which was dissolved in a saturated methanolic solution of zinc acetate (20 mL) and stirred at reflux for 30 min. The solvent was removed by evaporation, and CH_2Cl_2 (50 mL) was added to the residue, followed by washing with water (50 mL \times 3) and saturated brine (50 mL). After the mixture was dried over anhydrous Na_2SO_4 , the solvent was removed by evaporation. Purification of the residue by gel permeation chromatography afforded (*R*)-**1** as a dark-green solid (37.9 mg, 0.0569 mmol, 27%): mp 118–122 °C; ^1H NMR (500 MHz, CD_2Cl_2) δ 0.88 (t, $J = 7.6$ Hz, 3H for *M*-helix, CH_2CH_3), 1.09–1.22 (m, 12H for *P*-helix, $\text{CH}_2\text{CH}_3 \times 4$, and 9H for *M*-helix, $\text{CH}_2\text{CH}_3 \times 3$), 1.44 (d, $J = 6.4$ Hz, 3H for *P*-helix, PhC^*HCH_3), 1.58 (s, 3H for *M*-helix, CH_3), 1.65 (d, $J = 6.4$ Hz, 3H for *M*-helix, PhC^*HCH_3), 1.80 (s, 3H for *P*-helix, CH_3), 1.82 (m, 3H for *P*-helix and 3H for *M*-helix, CH_3), 2.03 (s, 3H for *P*-helix, CH_3), 2.04 (s, 3H for *M*-helix, CH_3), 2.10 (s, 3H for *P*-helix, CH_3), 2.11 (s, 3H for *M*-helix, CH_3), 2.44–2.62 (m, 8H for *P*-helix and 8H for *M*-helix, $\text{CH}_2\text{CH}_3 \times 4$), 5.46 (s, 1H for *M*-helix, meso-H), 5.71 (s, 1H for *P*-helix, meso-H), 6.21 (q, $J = 6.4$ Hz, 1H for *P*-helix, PhC^*HCH_3), 6.28 (q, $J = 6.4$ Hz, 1H for *M*-helix, PhC^*HCH_3), 6.47 (s, 1H for *P*-helix, meso-H), 6.55 (s, 1H for *M*-helix, meso-H), 6.56 (s, 1H for *P*-helix, meso-H), 6.60 (s, 1H for *M*-helix, meso-H), 7.18–7.33 (m, 5H for *P*-helix and 5H for *M*-helix, $\text{C}_6\text{H}_5\text{C}^*\text{HCH}_3$); IR (KBr) 2964, 2927, 2866, 1666, 1574, 1533, 1270, 1205, 743 cm^{-1} ; UV-vis (CH_2Cl_2 , 15 °C) $\epsilon_{404} = 30\,200$, $\epsilon_{785} = 15\,600\text{ M}^{-1}\text{ cm}^{-1}$; FAB MS m/z 664 ($[\text{M}]^+$); HR FAB MS calcd for $[\text{C}_{39}\text{H}_{44}\text{N}_4\text{O}_2\text{Zn}]^+$ 664.2756, found 664.2787. Anal. Calcd for $\text{C}_{39}\text{H}_{44}\text{N}_4\text{O}_2\text{Zn} \cdot \text{H}_2\text{O}$: C, 68.46; H, 6.78; N, 8.19. Found: C, 68.59; H, 6.72; N, 8.17.

Zinc Bilinones (*S*)-1, 2–10. Compounds **2–10** were prepared by the general procedure outlined above for (**(*R*)-1**).

[3,8,12,17-Tetraethyl-1,21-dihydro-2,7,13,18-tetramethyl-19-((*S*)-1-phenylethoxy)-(21*H*,24*H*)-1-bilinonato(2-)- $N^{21},N^{22},N^{23},N^{24}$]zinc(II) ((*S*)-1**).** A mixture of NaH (60% oil dispersion, 21.2 mg, 0.530 mmol), (*S*)-1-phenylethanol (70.2 mg, 0.575 mmol), and **11** (116 mg, 0.200 mmol) in dry THF (15 mL) was stirred for 20 h. The free base was purified by silica gel chromatography using $\text{CH}_2\text{Cl}_2/\text{MeOH}$ (100/1, v/v) as eluent. After zinc insertion, the yield of (**(*S*)-1**) was 31% (37.9 mg, 0.0569 mmol). Mp, ^1H NMR, IR, and UV-vis were identical with those reported for (**(*R*)-1**). HR FAB MS calcd for $[\text{C}_{39}\text{H}_{44}\text{N}_4\text{O}_2\text{Zn}]^+$ 664.2756, found 664.2778. Anal. Calcd for $\text{C}_{39}\text{H}_{44}\text{N}_4\text{O}_2\text{Zn} \cdot \text{H}_2\text{O}$: C, 68.46; H, 6.78; N, 8.19. Found: C, 68.23; H, 6.78; N, 8.07.

[3,8,12,17-Tetraethyl-1,21-dihydro-2,7,13,18-tetramethyl-19-((*R*)-1-(1-naphthyl)ethoxy)-(21*H*,24*H*)-1-bilinonato(2-)- $N^{21},N^{22},N^{23},N^{24}$]zinc(II) (2**).** A mixture of NaH (60% oil dispersion, 20.7 mg, 0.518 mmol), (*R*)-1-(1-naphthyl)ethanol (90.4 mg, 0.525 mmol), and **11** (116

(15) Riddick, J. A.; Bunger, W. B.; Sakano, T. K. *Organic Solvents*; Wiley and Sons: New York, 1986.

(16) Naruta, Y.; Tani, F.; Ishihara, N.; Maruyama, K. *J. Am. Chem. Soc.* **1991**, *113*, 6865–6872.

mg, 0.200 mmol) in dry THF (15 mL) was stirred for 1.5 h. Silica gel column chromatography was performed by using hexane/ethyl acetate (3/1, v/v) as eluent, followed by purification by silica gel thin-layer chromatography (hexane/ethyl acetate = 4/1, v/v as eluent). Treatment with a methanolic solution of zinc acetate was carried out at room temperature for 10 min. The yield of **2** was 29% (41.0 mg, 0.0572 mmol): mp 173–177 °C dec; ¹H NMR (500 MHz, CD₂Cl₂) δ 0.42 (t, *J* = 7.6 Hz, 3H for *M*-helix, CH₂CH₃), 1.00 (t, *J* = 7.6 Hz, 3H for *P*-helix, CH₂CH₃), 1.03–1.25 (m, 9H for *P*-helix and 9H for *M*-helix, CH₂CH₃ × 3), 1.43 (s, 3H for *M*-helix, CH₃), 1.60 (d, *J* = 6.4 Hz, 3H for *P*-helix, NaphC*HCH₃), 1.80 (d, *J* = 6.4 Hz, 3H for *M*-helix, NaphC*HCH₃), 1.81 (s, 3H for *P*-helix, CH₃), 1.87 (s, 3H for *M*-helix, CH₃), 1.88 (s, 3H for *M*-helix, CH₃), 1.91 (s, 3H for *P*-helix, CH₃), 1.92 (s, 3H for *P*-helix, CH₃), 2.07 (s, 3H for *M*-helix, CH₃), 2.18 (s, 3H for *P*-helix, CH₃), 2.37–2.64 (m, 8H for *P*-helix and 8H for *M*-helix, CH₂CH₃ × 4), 4.40 (s, 1H for *M*-helix, meso-H), 5.80 (s, H for the *P*-helix, meso-H), 6.38 (s, 1H for *P*-helix, meso-H), 6.39 (s, 1H for *P*-helix, meso-H), 6.44 (s, 1H for *M*-helix, meso-H), 6.54 (s, 1H for *M*-helix, meso-H), 7.12 (q, *J* = 6.4 Hz, 1H for *P*-helix, NaphC*HCH₃), 7.20 (q, *J* = 6.4 Hz, 1H for *M*-helix, NaphC*HCH₃), 7.28–8.04 (m, 7H for *P*-helix and 7H for *M*-helix, C₁₀H₇C*HCH₃); IR (KBr) 2964, 2924, 2866, 1662, 1574, 1531, 1269, 1205, 741 cm⁻¹; UV-vis (CH₂Cl₂, 15 °C) ε₄₀₇ = 30 700, ε₇₉₈ = 15 100 M⁻¹ cm⁻¹; FAB MS *m/z* 714 ([M]⁺); HR FAB MS calcd for [C₄₃H₄₆N₄O₂Zn]⁺ 714.2912, found 714.2877. Anal. Calcd for C₄₃H₄₆N₄O₂Zn: C, 72.11; H, 6.47; N, 7.82. Found: C, 71.82; H, 6.41; N, 8.04.

[3,8,12,17-Tetraethyl-1,21-dihydro-2,7,13,18-tetramethyl-19-((R)-1-(2-naphthyl)ethoxy)-(21H,24H)-1-bilironato(2-)-N²¹,N²²,N²³,N²⁴]-zinc(II) (3). A mixture of NaH (60% oil dispersion, 19.3 mg, 0.483 mmol), (*R*)-1-(2-naphthyl)ethanol (84.3 mg, 0.489 mmol), and **11** (116 mg, 0.200 mmol) in dry THF (15 mL) was stirred for 1.5 h. Silica gel column chromatography was performed by using hexane/ethyl acetate (3/1, v/v) as eluent, followed by purification by silica gel thin-layer chromatography (hexane/ethyl acetate = 4/1, v/v as eluent). Treatment with a methanolic solution of zinc acetate was carried out at room temperature for 10 min. The yield of **3** was 30% (43.0 mg, 0.0600 mmol): mp 148–152 °C dec; ¹H NMR (500 MHz, CD₂Cl₂) δ 0.63 (t, *J* = 7.6 Hz, 3H for *M*-helix, CH₂CH₃), 1.03–1.19 (m, 12H for *P*-helix, CH₂CH₃ × 4, and 9H for *M*-helix, CH₂CH₃ × 3), 1.49 (s, 3H for *M*-helix, CH₃), 1.51 (d, *J* = 6.4 Hz, 3H for *P*-helix, NaphC*HCH₃), 1.72 (d, *J* = 6.4 Hz, 3H for *M*-helix, NaphC*HCH₃), 1.82 (s, 3H for *P*-helix, CH₃), 1.84 (s, 3H for *P*-helix, CH₃), 1.86 (s, 3H for *M*-helix, CH₃), 1.96 (s, 3H for *P*-helix, CH₃), 2.02 (s, 3H for *M*-helix, CH₃), 2.10 (s, 3H for *M*-helix, CH₃), 2.12 (s, 3H for *P*-helix, CH₃), 2.42–2.72 (m, 8H for *P*-helix and 8H for *M*-helix, CH₂CH₃ × 4), 5.78 (s, 1H for *P*-helix, meso-H), 6.33 (q, *J* = 6.4 Hz, 1H for *P*-helix, NaphC*HCH₃), 6.42 (s, 1H for *P*-helix, meso-H), 6.49 (q, *J* = 6.4 Hz, 1H for *M*-helix, NaphC*HCH₃), 6.53 (s, 1H for *M*-helix, meso-H), 6.60 (s, 1H for *M*-helix, meso-H), 6.61 (s, 1H for *P*-helix, meso-H), 7.31–7.85 (m, 7H for *P*-helix and 7H for *M*-helix, C₁₀H₇C*HCH₃): (one meso proton for *M*-helix was masked by the signal of CHDCl₂); IR (KBr) 2966, 2924, 2866, 1662, 1574, 1531, 1269, 1205, 741 cm⁻¹; UV-vis (CH₂Cl₂, 15 °C) ε₄₀₄ = 32 000, ε₇₈₆ = 17 900 M⁻¹ cm⁻¹; FAB MS *m/z* 714 ([M]⁺); HR FAB MS calcd for [C₄₃H₄₆N₄O₂Zn]⁺ 714.2912, found 714.2880. Anal. Calcd for C₄₃H₄₆N₄O₂Zn·H₂O: C, 70.34; H, 6.59; N, 7.63. Found: C, 70.41; H, 6.39; N, 7.74.

[3,8,12,17-Tetraethyl-1,21-dihydro-2,7,13,18-tetramethyl-19-((R)-1-phenyl-1-butoxy)-(21H,24H)-1-bilironato(2-)-N²¹,N²²,N²³,N²⁴]-zinc(II) (4). A mixture of NaH (60% oil dispersion, 22.1 mg, 0.553 mmol), (*R*)-1-phenyl-1-butanol (75.1 mg, 0.500 mmol), and **11** (120 mg, 0.206 mmol) in dry THF (15 mL) was stirred for 13 h. Silica gel column chromatography was performed by using CH₂Cl₂ as eluent. The yield of **4** was 24% (34.4 mg, 0.0495 mmol): mp 114–118 °C; ¹H NMR (500 MHz, CD₂Cl₂) δ 0.65 (t, *J* = 7.6 Hz, 3H for *M*-helix, PhC*HCH₂-CH₃CH₃), 0.81 (t, *J* = 7.6 Hz, 3H for *P*-helix, PhC*HCH₂CH₃CH₃), 0.91–1.00 (m, 1H for *P*-helix, PhC*HCH₂CHHCH₃, and 2H for *M*-helix, PhC*HCH₂CH₂CH₃), 1.07–1.21 (m, 12H for *P*-helix, CH₂CH₃ × 4, and 12H for *M*-helix, CH₂CH₃ × 4), 1.25–1.32 (m, 1H for *P*-helix, PhC*HCH₂CHHCH₃), 1.55 (s, 3H for *M*-helix, CH₃), 1.60–1.77 (m, 2H for *P*-helix, PhC*HCH₂CH₂CH₃), 1.78 (s, 3H for *P*-helix, CH₃), 1.81 (s, 3H for *M*-helix, CH₃), 1.83 (s, 3H for *P*-helix, CH₃), 1.85–

2.00 (m, 2H for *M*-helix, PhC*HCH₂CH₂CH₃), 2.01 (s, 3H for *P*-helix, CH₃), 2.04 (s, 3H for *M*-helix, CH₃), 2.10 (s, 3H for *M*-helix, CH₃), 2.11 (s, 3H for *P*-helix, CH₃), 2.41–2.65 (m, 8H for *P*-helix and 8H for *M*-helix, CH₂CH₃ × 4), 5.51 (s, 1H for *M*-helix, meso-H), 5.72 (s, 1H for *P*-helix, meso-H), 5.85 (t, *J* = 6.7 Hz, 1H for *P*-helix, PhC*HPr), 6.09 (m, 1H for *M*-helix, PhC*HPr), 6.46 (s, 1H for *P*-helix, meso-H), 6.53 (s, 1H for *M*-helix, meso-H), 6.56 (s, 1H for *P*-helix, meso-H), 6.58 (s, 1H for *M*-helix, meso-H), 7.08–7.29 (m, 5H for *P*-helix and 5H for *M*-helix, C₆H₅C*HPr); IR (KBr) 2964, 2927, 2868, 1666, 1574, 1533, 1271, 1205, 743 cm⁻¹; UV-vis (CH₂Cl₂, 15 °C) ε₄₀₅ = 28 400, ε₇₈₄ = 15 500 M⁻¹ cm⁻¹; FAB MS *m/z* 692 ([M]⁺); HR FAB MS calcd for [C₄₁H₄₈N₄O₂Zn]⁺ 692.3069, found 692.3085. Anal. Calcd for C₄₁H₄₈N₄O₂Zn: C, 70.93; H, 6.97; N, 8.07. Found: C, 70.90; H, 7.04; N, 8.20.

[3,8,12,17-Tetraethyl-1,21-dihydro-2,7,13,18-tetramethyl-19-((R)-2-methyl-1-phenylpropoxy)-(21H,24H)-1-bilironato(2-)-N²¹,N²²,N²³,N²⁴]-zinc(II) (5). A mixture of NaH (60% oil dispersion, 19.1 mg, 0.478 mmol), (*R*)-2-methyl-1-phenyl-1-propanol (75.1 mg, 0.500 mmol), and **11** (116 mg, 0.200 mmol) in dry THF (15 mL) was stirred for 16 h. Silica gel column chromatography was performed by using CH₂Cl₂ as eluent. The yield of **5** was 26% (35.8 mg, 0.0516 mmol): mp 174–178 °C dec; ¹H NMR (500 MHz, CD₂Cl₂) δ 0.67–0.71 (m, 3H for *P*-helix, PhC*HCH(CH₃)CH₃, and 6H for *M*-helix, PhC*HCH(CH₃)-CH₃), 0.85 (d, *J* = 6.7 Hz, 3H for *P*-helix, PhC*HCH(CH₃)CH₃), 1.07–1.23 (m, 12H for *P*-helix and 12H for *M*-helix, CH₂CH₃ × 4), 1.47 (s, 3H for *M*-helix, CH₃), 1.77 (s, 3H for *P*-helix, CH₃), 1.88 (s, 3H for *P*-helix, CH₃), 1.92–1.99 (m, 1H for *P*-helix, PhC*HCH(CH₃)₂), 2.02 (s, 3H for *P*-helix, CH₃), 2.06 (s, 3H for *M*-helix, CH₃), 2.08 (s, 3H for *M*-helix, CH₃), 2.13 (s, 3H for *P*-helix, CH₃), 2.43–2.68 (m, 8H for *P*-helix and 8H for *M*-helix, CH₂CH₃ × 4), 5.43 (d, *J* = 7.6 Hz, 1H for *P*-helix, PhC*HPr), 5.46 (s, 1H for *M*-helix, meso-H), 5.79 (s, 1H for *P*-helix, meso-H), 6.02 (m, 1H for *M*-helix, PhC*HPr), 6.49 (s, 1H for *P*-helix, meso-H), 6.51 (s, 1H for *M*-helix, meso-H), 6.55 (s, 1H for *M*-helix, meso-H), 6.59 (s, 1H for *P*-helix, meso-H), 7.01–7.27 (m, 5H for *P*-helix and 5H for *M*-helix, C₆H₅C*HPr) (four protons (CH₃ × 1 and PhC*HCH(CH₃)₂ for *M*-helix) were not identified because they were probably masked by the signals of the *P*-helix protons); IR (KBr) 2964, 2929, 2870, 1664, 1572, 1533, 1271, 1207, 748 cm⁻¹; UV-vis (CH₂Cl₂, 15 °C) ε₄₀₆ = 31 400, ε₇₈₂ = 17 900 M⁻¹ cm⁻¹; FAB MS *m/z* 692 ([M]⁺); HR FAB MS calcd for [C₄₁H₄₈N₄O₂Zn]⁺ 692.3069, found 692.3036. Anal. Calcd for C₄₁H₄₈N₄O₂Zn·0.5H₂O: C, 70.02; H, 7.02; N, 7.97. Found: C, 69.94; H, 6.82; N, 8.14.

[3,8,12,17-Tetraethyl-1,21-dihydro-2,7,13,18-tetramethyl-19-((1R,2S)-2-phenyl-1-cyclohexyloxy)-(21H,24H)-1-bilironato(2-)-N²¹,N²²,N²³,N²⁴]-zinc(II) (6). A mixture of NaH (60% oil dispersion, 17.5 mg, 0.438 mmol), (*1R,2S*)-2-phenyl-1-cyclohexanol (70.7 mg, 0.401 mmol), and **11** (116 mg, 0.200 mmol) in dry THF (15 mL) was stirred for 48 h. Silica gel column chromatography was performed by using CH₂Cl₂/MeOH (100/1, v/v) as eluent. The yield of **6** was 31% (40.7 mg, 0.0621 mmol): mp 109–113 °C; ¹H NMR (500 MHz, CD₂Cl₂) δ 1.02 (t, *J* = 7.6 Hz, 3H for *P*-helix, CH₂CH₃), 1.13–1.26 (m, 11H for *P*-helix, CH₂CH₃ × 3 and cyclohexyl-H × 2, and 14H for *M*-helix, CH₂CH₃ × 4 and cyclohexyl-H × 3), 1.44–1.55 (m, 3H for *P*-helix, cyclohexyl-H × 3, and 2H for *M*-helix, cyclohexyl-H × 2), 1.58 (s, 3H for *M*-helix, CH₃), 1.66–1.82 (m, 9H for *P*-helix, CH₃ × 2 and cyclohexyl-H × 3, and 6H for *M*-helix, CH₃ and cyclohexyl-H × 3), 2.08 (s, 3H for *P*-helix, CH₃), 2.11 (m, 3H for *P*-helix, CH₃ and 6H for *M*-helix, CH₃ × 2), 2.32–2.75 (m, 9H for *P*-helix and 9H for *M*-helix, CH₃CH₂ × 4 and cyclohexyl-H), 4.71 (dt, *J* = 4.0, 10.4 Hz, H for *M*-helix, cyclohexyl-H), 5.03 (dt, *J* = 3.1, 9.8 Hz, 1H for cyclohexyl-H), 5.72 (s, 1H for *P*-helix, meso-H), 5.85 (s, 1H for *M*-helix, meso-H), 6.21 (s, 1H for *P*-helix, meso-H), 6.56–6.60 (m, 2H for *P*-helix and 2H for *M*-helix, phenyl-H × 2), 6.63 (s, 1H for *M*-helix, meso-H), 6.69 (s, 1H for *M*-helix, meso-H), 6.72 (s, 1H for *P*-helix, meso-H), 6.88 (dd, *J* = 1.5, 7.3 Hz, 2H for *P*-helix, phenyl-H × 2), 6.99 (dd, *J* = 1.5, 7.3 Hz, 2H for *M*-helix, phenyl-H × 2), 7.11–7.16 (m, 1H for *P*-helix and 1H for *M*-helix, phenyl-H); IR (KBr) 2964, 2929, 2864, 1666, 1574, 1533, 1273, 1205, 1149, 746 cm⁻¹; UV-vis (CH₂Cl₂, 15 °C) ε₄₀₃ = 29 100, ε₇₈₃ = 18 000 M⁻¹ cm⁻¹; FAB MS *m/z* 718 ([M]⁺); HR FAB MS calcd for [C₄₃H₅₀N₄O₂Zn]⁺ 718.3225, found

718.3226. Anal. Calcd for $C_{43}H_{50}N_4O_2Zn \cdot H_2O$: C, 69.95; H, 7.10; N, 7.59. Found: C, 70.07; H, 7.30; N, 7.19.

[3,8,12,17-Tetraethyl-1,21-dihydro-2,7,13,18-tetramethyl-19-((R)-2,2'-dimethoxy-1,1'-binaphthalen-3-ylmethoxy)-(21H,24H)-1-bilidonato(2-)- $N^{21},N^{22},N^{23},N^{24}$]zinc(II) (7). A mixture of NaH (60% oil dispersion, 14.4 mg, 0.360 mmol), (R)-2,2'-dimethoxy-1,1'-binaphthalen-3-ylmethanol (51.6 mg, 0.150 mmol), and **11** (87.1 mg, 0.150 mmol) in dry THF (10 mL) was stirred for 6 h. Silica gel column chromatography was performed by using CH_2Cl_2 as eluent. The yield of **7** was 27% (36.4 mg, 0.0410 mmol): mp 172–176 °C dec; 1H NMR (500 MHz, CD_2Cl_2) δ 0.99 (t, $J = 7.6$ Hz, 3H, CH_2CH_3), 1.07–1.13 (m, 15H, $CH_2CH_3 \times 5$), 1.17–1.21 (m, 6H, $CH_2CH_3 \times 2$), 1.78 (m, 6H, $CH_3 \times 2$), 1.79 (s, 3H, CH_3), 1.81 (s, 3H, CH_3), 1.88 (s, 3H, CH_3), 1.93 (s, 3H, CH_3), 2.07 (m, 6H, $CH_3 \times 2$), 2.19 (q, $J = 7.6$ Hz, 2H, CH_2CH_3), 2.33–2.42 (m, 2H, CH_2CH_3), 2.49–2.56 (m, 12H, $CH_2CH_3 \times 6$), 3.19 (m, 6H, OMe $\times 2$), 3.78 (s, 3H, OMe), 3.82 (s, 3H, OMe), 5.49 (s, 1H, meso-H), 5.53 (s, 1H, meso-H), 5.70 (d, $J = 11.6$ Hz, 1H, -CHHO-), 5.76 (d, $J = 11.6$ Hz, 1H, -CHHO-), 6.09 (d, $J = 11.6$ Hz, 1H, -CHHO-), 6.15 (d, $J = 11.6$ Hz, 1H, -CHHO-), 6.50 (s, 1H, meso-H), 6.51 (s, 1H, meso-H), 6.56 (m, 2H, meso-H $\times 2$), 7.02–7.09 (m, 4H, binaphthyl-H $\times 4$), 7.19–7.24 (m, 4H, binaphthyl-H $\times 4$), 7.30–7.33 (m, 2H, binaphthyl-H $\times 2$), 7.34–7.40 (m, 2H, binaphthyl-H $\times 2$), 7.47–7.50 (m, 2H, binaphthyl-H $\times 2$), 7.81–7.82 (m, 2H, binaphthyl-H $\times 2$), 7.87–7.90 (m, 4H, binaphthyl-H $\times 4$), 8.03–8.05 (m, 2H, binaphthyl-H $\times 2$) (assignment of the signals to the *P*- and *M*-isomers was not achieved because of the low diastereomeric excess); IR (KBr) 2964, 2931, 2868, 1659, 1597, 1574, 1535, 1205, 746 cm^{-1} ; UV-vis (CH_2Cl_2 , 15 °C) $\epsilon_{406} = 30\,300$, $\epsilon_{785} = 15\,900$ $M^{-1}cm^{-1}$; FAB MS m/z 887 ($[M + H]^+$); HR FAB MS calcd for $[C_{54}H_{54}N_4O_4Zn]^{+}$ 886.3437, found 886.3443. Anal. Calcd for $C_{54}H_{54}N_4O_4Zn \cdot H_2O$: C, 71.55; H, 6.23; N, 6.18. Found: C, 71.63; H, 6.07; N, 6.13.

[19-((S)-2-Butoxy)-3,8,12,17-tetraethyl-1,21-dihydro-2,7,13,18-tetramethyl-(21H,24H)-1-bilidonato(2-)- $N^{21},N^{22},N^{23},N^{24}$]zinc(II) (8). A mixture of NaH (60% oil dispersion, 20.0 mg, 0.500 mmol), (S)-2-butanol (37.1 mg, 0.500 mmol), and **11** (118 mg, 0.204 mmol) in dry THF (15 mL) was stirred for 16 h. Silica gel column chromatography was performed by using hexane/ethyl acetate (1/2, v/v) as eluent. Treatment with a methanolic solution of zinc acetate (20 mL) was carried out at room temperature for 15 min. The yield of **8** was 25% (31.0 mg, 0.0501 mmol): mp 227–231 °C; 1H NMR (500 MHz, CD_2Cl_2) δ 0.72 (t, $J = 7.6$ Hz, 3H, $CH_3CH_2C^*HCH_3$), 0.83 (t, $J = 7.6$ Hz, 3H, $CH_3CH_2C^*HCH_3$), 1.07–1.21 (m, 27H, $CH_2CH_3 \times 8$ and $CH_3-CH_2C^*HCH_3$), 1.28 (d, $J = 6.4$ Hz, 3H, $CH_3CH_2C^*HCH_3$), 1.48–1.62 (m, 2H, $CH_3CH_2C^*HCH_3$, and 1H, $CH_3CHHC^*HCH_3$), 1.73–1.81 (m, 13H, $CH_3 \times 4$, and $CH_3CHHC^*HCH_3$), 2.03 (s, 6H, $CH_3 \times 2$), 2.08 (s, 6H, $CH_3 \times 2$), 2.38–2.56 (m, 16H, $CH_2CH_3 \times 8$), 5.08 (m, 1H, $CH_3CH_2C^*HCH_3$), 5.23 (m, 1H, $CH_3CH_2C^*HCH_3$), 5.59 (s, 1H, meso-H), 5.60 (s, 1H, meso-H), 6.53–6.55 (m, 4H, meso-H $\times 4$) (assignment of the signals to the *P*- and *M*-isomers was not achieved because of the low diastereomeric excess); IR (KBr) 2966, 2926, 2868, 1660, 1572, 1533, 1205, 741 cm^{-1} ; UV-vis (CH_2Cl_2 , 15 °C) $\epsilon_{401} = 36\,400$, $\epsilon_{776} = 19\,100$ $M^{-1}cm^{-1}$; FAB MS m/z 616 ($[M]^+$); HR FAB MS calcd for $[C_{35}H_{44}N_4O_2Zn]^{+}$ 616.2756, found 616.2783. Anal. Calcd for $C_{35}H_{44}N_4O_2Zn$: C, 68.01; H, 7.18; N, 9.06. Found: C, 68.37; H, 7.09; N, 9.35.

[3,8,12,17-Tetraethyl-1,21-dihydro-2,7,13,18-tetramethyl-19-((S)-3-methyl-2-butoxy)-(21H,24H)-1-bilidonato(2-)- $N^{21},N^{22},N^{23},N^{24}$]zinc(II) (9). A mixture of NaH (60% oil dispersion, 22.8 mg, 0.570 mmol), (S)-3-methyl-2-butanol (44.6 mg, 0.506 mmol), and **11** (116 mg, 0.200 mmol) in dry THF (15 mL) was stirred for 18 h. Silica gel column

chromatography was performed by using $CH_2Cl_2/MeOH$ (100/1, v/v) as eluent. The yield of **9** was 41% (51.8 mg, 0.0819 mmol): mp 230–234 °C; 1H NMR (500 MHz, CD_2Cl_2) δ 0.69 (d, $J = 7.0$ Hz, 3H, $CH_3C^*HCH(CH_3)_2$), 0.76 (d, $J = 7.0$ Hz, 3H, $CH_3C^*HCH(CH_3)_2$), 0.82–0.84 (m, 6H, $CH_3C^*HCH(CH_3)_2 \times 2$), 1.03 (d, $J = 6.4$ Hz, 3H, $CH_3C^*HCH(CH_3)_2$), 1.11–1.19 (m, 24H, $CH_2CH_3 \times 8$), 1.23 (d, $J = 6.4$ Hz, 3H, $CH_3C^*HCH(CH_3)_2$), 1.71–1.76 (m, 13H, $CH_3 \times 4$ and $CH_3C^*HCH(CH_3)_2$), 2.03 (s, 3H, CH_3), 2.04 (s, 3H, CH_3), 2.09 (s, 3H, CH_3), 2.10 (s, 3H, CH_3), 2.14–2.18 (m, 1H, $CH_3C^*HCH(CH_3)_2$), 2.39–2.60 (m, 16H, $CH_2CH_3 \times 8$), 4.81 (m, 1H, $CH_3C^*HCH(CH_3)_2$), 5.14 (m, 1H, $CH_3C^*HCH(CH_3)_2$), 5.63 (s, 2H, meso-H $\times 2$), 6.56 (s, 2H, meso-H $\times 2$), 6.58 (s, 1H, meso-H), 6.59 (s, 1H, meso-H) (the signals of the *P*-isomer are not reported since not all signals were observed due to the low diastereomeric excess); IR (KBr) 2966, 2924, 2868, 1660, 1574, 1533, 1205, 737 cm^{-1} ; UV-vis (CH_2Cl_2 , 15 °C) $\epsilon_{402} = 34\,500$, $\epsilon_{776} = 19\,200$ $M^{-1}cm^{-1}$; FAB MS m/z 630 ($[M]^+$); HR FAB MS calcd for $[C_{36}H_{46}N_4O_2Zn]^{+}$ 630.2912, found 630.2912. Anal. Calcd for $C_{36}H_{46}N_4O_2Zn \cdot H_2O$: C, 66.50; H, 7.44; N, 8.62. Found: C, 66.83; H, 7.46; N, 8.52.

[3,8,12,17-Tetraethyl-1,21-dihydro-2,7,13,18-tetramethyl-19-((1R,2S,5R)-5-methyl-2-isopropyl-1-cyclohexoxy)-(21H,24H)-1-bilidonato(2-)- $N^{21},N^{22},N^{23},N^{24}$]zinc(II) (10). A mixture of NaH (60% oil dispersion, 22.0 mg, 0.550 mmol), (1R,2S,5R)-5-methyl-2-isopropyl-1-cyclohexanol (L-(–)-menthol, 87.0 mg, 0.557 mmol), and **11** (116 mg, 0.200 mmol) in dry THF (15 mL) was stirred for 20 h. Silica gel column chromatography was performed by using CH_2Cl_2 as eluent. The yield of **10** was 38% (53.1 mg, 0.0758 mmol): mp 224–228 °C dec; 1H NMR (500 MHz, CD_2Cl_2) δ 0.53–0.54 (m, 3H for *P*-helix and 3H for *M*-helix, menthyl- CH_3), 0.61 (d, $J = 7.0$ Hz, 3H for *P*-helix, menthyl- $CH(CH_3)CH_3$), 0.69–0.96 (m, 6H for *P*-helix, menthyl-H $\times 3$ and menthyl- $CH(CH_3)CH_3$, and 9H for *M*-helix, menthyl-H $\times 3$ and menthyl- $CH(CH_3)CH_3$), 1.06–1.47 (m, 14H for *P*-helix and 14H for *M*-helix, menthyl-H $\times 2$ and $CH_2CH_3 \times 4$), 1.49–1.68 (m, 2H for *P*-helix, and 2H for *M*-helix, menthyl-H $\times 2$), 1.69–1.76 (m, 3H for *P*-helix, CH_3 , and 7H for *M*-helix, menthyl-H and $CH_3 \times 2$), 1.80 (s, 3H for *P*-helix, CH_3), 1.83–1.89 (m, 1H for *P*-helix, menthyl-H), 2.05 (s, 3H for *M*-helix, CH_3), 2.08 (s, 3H for *P*-helix, CH_3), 2.10 (s, 3H for *M*-helix, CH_3), 2.13 (s, 3H for *P*-helix, CH_3), 2.36–2.48 (m, 2H for *P*-helix, CH_2CH_3 , and 3H for *M*-helix, CH_2CH_3 and menthyl-H), 2.52–2.66 (m, 7H for *P*-helix, $CH_2CH_3 \times 3$ and menthyl-H, and 6H for *M*-helix, $CH_2CH_3 \times 3$), 4.46 (m, 1H for *P*-helix, menthyl- $CH-O$), 4.78 (m, 1H for *P*-helix, menthyl- $CH-O$), 5.65 (s, 1H for *M*-helix, meso-H), 5.75 (s, 1H for *P*-helix, meso-H), 6.58 (s, 1H for *M*-helix, meso-H), 6.60 (s, 1H for *M*-helix, meso-H), 6.67 (s, 1H for *P*-helix, meso-H), 6.68 (s, 1H for *P*-helix, meso-H); IR (KBr) 2962, 2927, 2868, 1660, 1574, 1533, 1209, 744 cm^{-1} ; UV-vis (CH_2Cl_2 , 15 °C) $\epsilon_{402} = 32\,900$, $\epsilon_{774} = 21\,200$ $M^{-1}cm^{-1}$; FAB MS m/z 698 ($[M]^+$); HR FAB MS calcd for $[C_{41}H_{54}N_4O_2Zn]^{+}$ 698.3538, found 698.3569. Anal. Calcd for $C_{41}H_{54}N_4O_2Zn \cdot H_2O$: C, 68.56; H, 7.86; N, 7.80. Found: C, 68.57; H, 7.93; N, 7.76.

Acknowledgment. This work was supported by a Grant-in-Aid for Scientific Research from the Ministry of Education, Science, Sports, and Culture, Japan. We appreciate Professor Hiroyuki Nakazumi for his kind help in IR studies. We thank Tadao Kobatake for help in mass spectroscopic studies. Ab initio calculations were performed in the Supercomputer Laboratory, Institute for Chemical Research, Kyoto University.

JA9830849